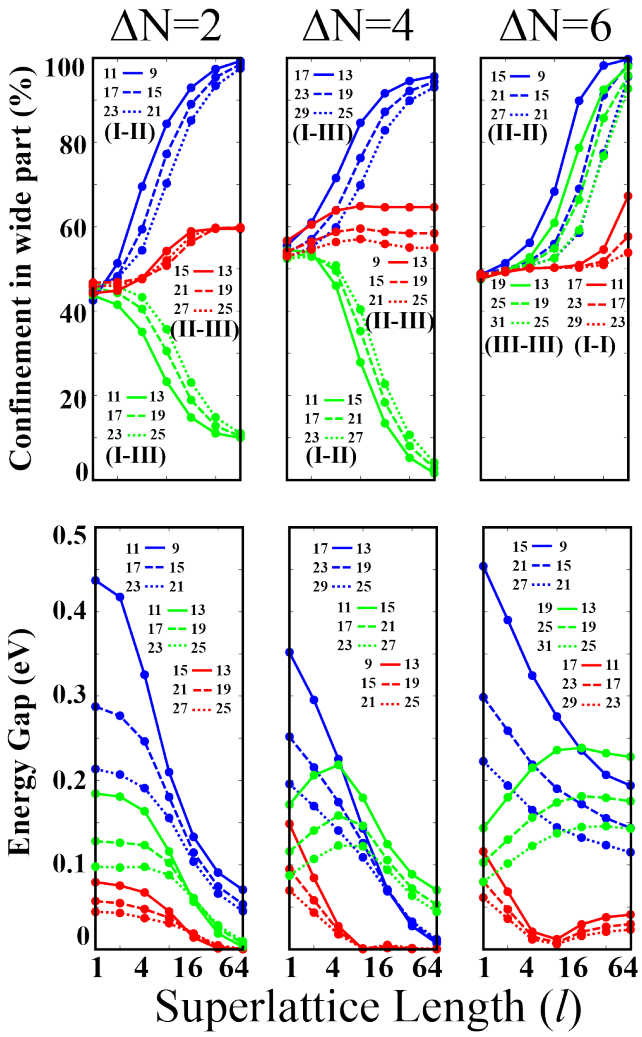

FIG. 5. Variation of confinements and energy gaps of superlattices with the lengths of constituent parts. Results are derived by the tight binding model described in the text. Numbers labelling the curves correspond to n_1 and n_2. The lengths, l, of the constituent parts are equal and shown in the logarithmic scale.

V. SUPERLATTICES

In this section we investigate the electronic structure of superlattices formed by periodic junction of ASiNRs which have different widths. The variation of energy gaps with the ribbon width causes these structures act as a multiple quantum well and is expected to lead to interesting device applications. In the past, superlattices of 2D GaAs-AlAs or Si-Ge heterostructures have been extensively studied to realize new generation electronic devices. Recently, superlattices of graphene have been synthesized experimentally.[31] The transport characteristics and electron confinement have been revealed.[32] Here superlattices are formed by the junction of two different nanoribbons. In this study the lengths of constituent nanoribbons are taken to be equal. The unequal cases were studied for armchair nanoribbons of graphene.[11] We let l unit cell of a ribbon with the width of n_1 to make a perfect junction with l unit cell of a ribbon with the width of n_2; once joined these structures form a supercell having the length of $2l$. Here n_1 and n_2 are chosen to be odd, so that the ribbons are joined symmetrically. Then the resulting structure is relaxed and the lattice constant of the whole structure is determined. This superlattice structure is labelled by its dimensions as SL$(n_1, n_2; l)$. The indices 1 and 2 are arranged in a way that a ribbon with a width n_1 has smaller band gap than a ribbon with a width n_2. The width difference $\Delta N = n_1 - n_2$ is defined for classification purpose.

Figure 4 presents the band structure and projected charge density isosurface plots for sample superlattices having $\Delta N = 2$ and 4 calculated by DFT. The band profile is nearly symmetric around the Fermi level and one can easily track the bonding and antibonding states from the charge density profile. As seen in the charge density plots, the band edge states of SL$(11, 9; 4)$ and SL$(11, 13; 4)$ superlattices are confined in the wide and narrow part, respectively. This can be explained by taking into account the band gaps of constituent ribbons of superlattice structures. Due to the symmetry between valence and conduction band edges of the constituent ribbons, the superlattice band line-up is always normal. As a result, the part having lower gap acts as a quantum well for electrons and holes. That is why, the electrons of SL$(11, 9; 4)$ and SL$(11, 13; 4)$ structures are confined in the $n = 11$ part, which for both superlattices is the part having the smaller energy gap.

The situation is also similar for the structures having $\Delta N = 4$. Electrons of SL$(17, 13; 4)$ and SL$(11, 15; 4)$ are confined, respectively, in the wide and narrow part, which has the lower energy gap. Moreover, the superlattices constructed by the nanoribbons, which are members of the same family, have similar electronic structure. In Fig. 4 the superlattices having such common property are shown in the same column. Here one can see the similarity in the energy band profile of these structures. Another way to construct such structures is to increase the width of both constituent parts by $n = 6k$. To verify this, we have calculated the electronic structure of SL$(17, 15; 4)$ and SL$(17, 19; 4)$, which yielded in the similar results as that of SL$(11, 9; 4)$ and SL$(11, 13; 4)$, except that in former structures the confinements are less pronounced because the band gap difference is lower.

We have to mention that, even though the structures SL$(9, 13; 4)$ and SL$(15, 13; 4)$ have a considerable band gap difference between constituent parts, they do not have confinement neither in the wide nor in the narrow part. This is related to the interface effects, which will be discussed in a frame of another simple model.

Calculations for larger structures with *ab initio* techniques are computationally too expensive. So we have used the tight binding model mentioned before. In Fig.4 one can see that, the tight binding model can reproduce the band edge profiles over the whole Brillouin zone.